Am J Physiol Cell Physiol 283: C1637–C1645, 2002.
First published August 14, 2002; 10.1152/ajpcell.00266.2002.

TRPC4 currents have properties similar to the pacemaker current in interstitial cells of Cajal

REBECCA L. WALKER,* SANG DON KOH,* GERARD P. SERGEANT, KENTON M. SANDERS, AND BURTON HOROWITZ
Department of Physiology and Cell Biology, University of Nevada, School of Medicine, Reno, Nevada 89557

Received 7 June 2002; accepted in final form 9 August 2002

Walker, Rebecca L., Sang Don Koh, Gerard P. Sergeant, Kenton M. Sanders, and Burton Horowitz. TRPC4 currents have properties similar to the pacemaker current in interstitial cells of Cajal. *Am J Physiol Cell Physiol* 283: C1637–C1645, 2002. First published August 14, 2002; 10.1152/ajpcell.00266.2002.—Interstitial cells of Cajal (ICC) are the pacemaker cells responsible for the generation and propagation of electrical slow waves in phasic muscles of the gastrointestinal (GI) tract. The pacemaker current that initiates each slow wave derives from a calcium-inhibited, voltage-independent, nonselective cation channel. This channel in ICC displays properties similar to that reported for the transient receptor potential (TRP) family of nonselective cation channels, particularly those seen for TRPC3 and TRPC4. We have identified transcripts for TRPC4 in individually isolated ICC and have cloned the two alternatively spliced forms of TRPC4, TRPC4α and TRPC4β, from GI muscles. TRPC4β is missing an 84-amino acid segment from the carboxy terminus. Expression of either form using the whole cell patch-clamp technique led to calcium-inhibited, nonselective cation channels as determined by *N*-methyl-D-glucamine replacement experiments and BAPTA dialysis. Expression of TRPC4β channels recorded at the whole cell level had characteristics similar to the nonselective cation current in ICC. The single-channel conductance of TRPC4β was determined to be 17.5 pS. Application of calmidazolium to cells expressing TRPC4β led to a significant increase in the inward current of these cells at both the whole cell and single-channel level, and currents were sensitive to block by 10 μM lanthanum, niflumic acid, and DIDS. Comparison of the properties reported for the nonselective cation current in ICC and those identified here for TRPC4β led us to conclude that a TRPC4-like current encodes the plasmalemmal pacemaker current in murine small intestine.

cation channel; gastrointestinal; smooth muscle; calmodulin

INTERSTITIAL CELLS OF CAJAL (ICC) are the pacemaking cells in gastrointestinal (GI) muscles that generate the rhythmic oscillations in membrane potential known as slow waves (7, 16). Slow waves propagate within ICC networks, conduct into smooth muscle cells via gap junctions, and initiate phasic contractions via activation of Ca^{2+} entry through L-type Ca^{2+} channels. Ablation of ICC networks by genetic means (25) or through inactivation of Kit receptors with neutralizing antibodies (21) results in elimination of slow wave activity and alterations in GI motility. The pacemaker mechanism has been shown to involve rhythmic oscillations in intracellular calcium concentration ($[Ca^{2+}]_i$) in a compartment near the plasma membrane that controls the open probability of channels responsible for pacemaker currents. This mechanism involves Ca^{2+} release from D-*myo*-inositol 1,4,5-trisphosphate (IP_3) receptor-operated stores and uptake of Ca^{2+} by mitochondria (26). Mitochondrial Ca^{2+} uptake activates voltage-independent, Ca^{2+}-inhibited, nonselective cation channels with a unitary conductance of 13 pS (10). The molecular species responsible for the pacemaker conductance has not been identified.

Transient receptor potential (TRP) channels were first cloned from *Drosophila* (TRP and TRPL) and constitute a superfamily of proteins encoding a diverse group of Ca^{2+}-permeable cation channels (14). One subfamily, the classic or canonical TRPs, has seven members (TRPC1–7) and participates in functions as diverse as store-operated Ca^{2+} entry (4), vasorelaxation (2), and egg fertilization (8). Some of the characteristics of the Ca^{2+}-inhibited, nonselective cation currents in ICC (10) are similar to those of TRPC3 and TRPC4 currents. Transcripts for both TRPC4 and TRPC6 have been identified in freshly dispersed ICC (1), but transcripts for TRPC3 have not been identified in this cell type (23). TRPC4 exists as two alternatively spliced transcripts that are expressed in several tissue and cell types (15, 23). TRPC4α represents the complete form of the protein, whereas TRPC4β is missing an 84-amino acid segment from the carboxy terminus (13, 17). TRPC4α, originally cloned from bovine retina, was shown to activate upon application of GTPγs or depletion of intracellular calcium stores (15). Recently, Schaefer et al. (17) reported the expression of TRPC4α and TRPC4β, demonstrating the receptor-dependent, but store-independent, activation of these channels in HEK-293 cells. In addition, two independent studies by Tang et al. (19) and Trost et al. (22) examined the

* R. L. Walker and S. D. Koh contributed equally to this work.

Address for reprint requests and other correspondence: B. Horowitz, Dept. of Physiology and Cell Biology, Univ. of Nevada, School of Medicine, Reno, NV 89557 (E-mail: burt@physio.unr.edu).

The costs of publication of this article were defrayed in part by the payment of page charges. The article must therefore be hereby marked "*advertisement*" in accordance with 18 U.S.C. Section 1734 solely to indicate this fact.

calmodulin-binding sites of TRPC4 and reported the Ca^{2+}-dependent binding of calmodulin at two locations in the cytosolic COOH terminus of TRPC4α and one in TRPC4β. We have previously reported the cloning of TRPC4α and TRPC4β from murine colonic smooth muscle tissues (23).

In the present study, we examined the properties of TRPC4 splice variants (TRPC4α and TRPC4β) to determine whether either isoform could be responsible for the Ca^{2+}-inhibited, nonselective cation (pacemaker) conductance in ICC. We expressed TRPC4α and TRPC4β in HEK-293 cells and used the patch-clamp technique to examine the properties of TRPC4 whole cell and unitary currents. The effects of calmidazolium (CMZ), a calmodulin inhibitor, were tested on whole cell and single-channel currents. The properties of TRPC4β were remarkably like the pacemaker conductance and led us to conclude that slow wave activity in murine GI muscles may be due to a TRPC4-like conductance.

MATERIALS AND METHODS

Molecular techniques:RT-PCR. Total RNA was prepared from cell cultures by using the Trizol reagent (Invitrogen, San Diego, CA) as per manufacturer's instruction. First strand cDNA was prepared from the RNA preparations by using the Superscript II reverse transcriptase kit (GIBCO BRL, Gaithersberg, MD), and 500 μg/μl of oligo dT primers were used to reverse transcribe the RNA sample. The cDNA reverse transcription product was amplified with specific primers by PCR as previously described (23). The following PCR primers were used (the first number represents the sense-bordering nucleotide positions, the second number represents the antisense-bordering nucleotide positions, and the number in parenthesis is the GenBank accession number): TRPC4 primers (AF019663) nt 1667–1686 and 1742–1760, amplicon = 93 bp, will amplify both α and β forms of TRPC4; and TRPC4 wild-type primers (AF019663) nt 2518–2538 and 2599–2620, amplicon = 102 bp, will amplify only the α form of TRPC4 and not the alternatively spliced β form, because the primers were designed to hybridize to the deleted region in the alternatively spliced transcript.

Adenoviral constructs. Constructs used for expression in HEK-293 cells were developed in the pcDNA3.1 mammalian expression vector (Invitrogen, San Diego, CA). Plasmid DNA was prepared from overnight cultures by using the Qiagen Miniprep kit and sequenced by the ABI Prism 310 genetic analyzer (Applied Biosytems, Foster City, CA) to confirm the correct plasmid construct. Recombinant adenoviruses for TRPC4α and TRPC4β were then produced, purified, and amplified by using the AdEasy adenoviral vector system (Stratagene, La Jolla, CA) and were used to infect HEK-293 cells. The virus without any recombinant insert (GFP) was used as a control. Viral production and infection of cells are aided by the presence of green fluorescent protein (GFP) encoded by a gene incorporated into the viral backbone. For infection, HEK-293 cells were plated 24 h before viral infection. TRP viral constructs were added to the cells with fresh growth medium. Infected cells can be monitored by observing how many cells are green under fluorescent microscopy at 24 and 48 h and were subsequently used in electrophysiological recordings and for molecular analysis.

Cell cultures. HEK-293 cells (ATCC, Manassas, VA) were obtained and cultured in low-glucose DMEM (Invitrogen, San Diego, CA) with 10% FBS. Cells were passaged weekly, and fresh medium was applied every 2–3 days.

Creation of TRPC4 stable lines. TRPC4α and TRPC4β were cloned from murine colonic smooth muscle as previously described (23) and ligated into pcDNA3.1 mammalian vector (Invitrogen). Clones in this vector were used to generate stable lines in HEK-293 cells by use of the calcium phosphate method and G418 selection (Invitrogen). PCR analysis and whole cell patch-clamp recordings confirmed stable lines.

Voltage-clamp experiments in HEK-293 cells. The patch-clamp technique for whole cell recording was utilized in these experiments. The patch pipettes were made from borosilicate glass capillaries pulled with micropipette puller (P-80/PC, Sutter, CA) and heat polished with a microforge (MF-83, Narishige, Japan). The pipette resistances were 1–3 MΩ for whole cell recordings and 5–8 MΩ for single-channel recordings. The average cell capacitance was 17 ± 1 pA. Currents were amplified with a List EPC-7 amplifier and/or Axopatch-1A amplifier and digitized with a 12-bit analog-to-digital converter (Digidata 1322A; Axon instrument, Foster City, CA). The data were stored directly and digitized online by using pCLAMP software (version 8.0; Axon instrument). Data were sampled at 2 kHz for whole cell and 5 kHz for single-channel recordings and filtered at 1 kHz using an 8-pole Bessel filter. Data were analyzed using pCLAMP (version 8.0; Axon Instrument), GraphPad Prizm (version 3.0; San Diego, CA), and Origin software (MicroCal Software, version 5.0; Northampton, MA).

Solutions. The bath solution, Ca^{2+}-phosphate-buffered saline (PSS), contained (in mM) 5 KCl, 135 NaCl, 2 $CaCl_2$, 10 glucose, 1.2 $MgCl_2$, and 10 HEPES, pH 7.4, with Tris. The pipette solutions contained (in mM) 110 Cs aspartate, 30 TEA-Cl, 5 $MgCl_2$, 2.7 K_2ATP, 0.1 Na_2GTP, 2.5 creatine phosphate disodium salt, 10 BAPTA, and 5 HEPES, pH 7.2, with Tris. BAPTA (10 mM) was replaced with EGTA (0.1 mM) in some experiments to raise intracellular free Ca^{2+}. Na^+ replacement was performed by replacing equimolar amounts of *N*-methyl-D-glucamine ($NMDG^+$). For single-channel recordings, pipette solutions for on-cell and excised patches were Ca^{2+}-PSS. The bath solution for on-cell patches contained (in mM) 140 KCl, 1 EGTA, 0.61 $CaCl_2$, and 10 HEPES adjusted to pH 7.4 with Tris. To test the Ca^{2+} sensitivity of channels in the excised patches, the bath solution contained (in mM) 110 potassium gluconate, 30 KCl, 1 EGTA, and 10 HEPES adjusted to pH 7.4 with Tris. Ca^{2+} was added to a bath solution buffered by 1 mM EGTA to create Ca^{2+} activities from 10^{-7} to 10^{-6} M. Activities were calculated with a program developed by C. M. Hai (University of Virginia, Charlottesville, VA). $LaCl_3$ (La^{3+}) (Sigma, St Louis, MO) was dissolved into water. CMZ, niflumic acid, and DIDS were dissolved into DMSO to prepare stock solutions (10^{-1} M) and were added to the bath solution in some experiments. All experiments were performed at room temperature.

Statistical analysis. Data are expressed as means ± SE. The "*n* values" in the text indicate the number of cells used in whole cell patch-clamp experiments or the number of membrane patches used in single-channel analysis. *P* values <0.05 were taken as a statistically significant difference.

RESULTS

Molecular features of TRP channels. Full-length cDNAs of TRPC4α and TRPC4β were amplified from murine colonic smooth muscle RNA by using gene-specific primers (23). These cDNAs were used to produce a stable line of HEK-293 cells expressing TRPC4β, as well as TRPC4α and TRPC4β adenovi-

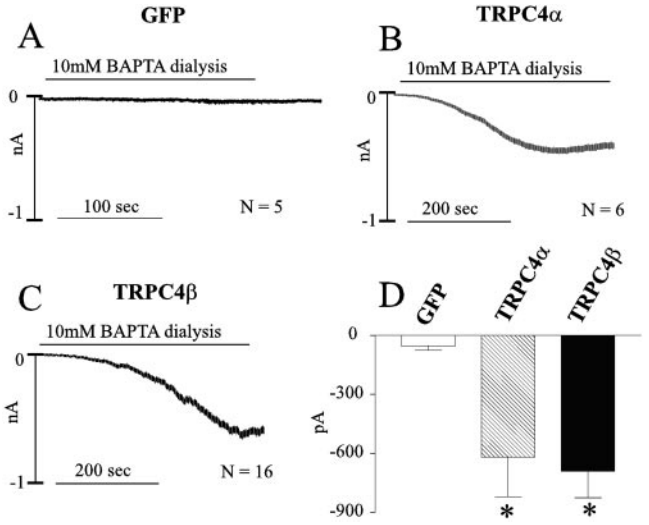

Fig. 1. Effects of BAPTA dialysis on TRPC4α and TRPC4β expressed in HEK-293 cells. Currents were recorded by using the whole cell patch-clamp technique. *A*: dialysis with 10 mM BAPTA induced a small inward current in HEK-293 cells infected with a virus expressing green fluorescent protein (GFP) only. *B*: the current generated in HEK cells stably transfected with TRPC4α. Dialysis with BAPTA generates a larger current in these cells compared with control HEK cells. *C*: the current generated in HEK cells infected with TRPC4β virus. Dialysis with BAPTA generates a current in cells expressing TRPC4β. *D*: data from HEK-293 cells alone, HEK cells + TRPC4α, and HEK cells + TRPC4β are summarized. *Statistically significant difference compared with control infected cells, $P < 0.05$.

ruses for use in transient infections of cells (see MATERIALS AND METHODS). Calmodulin-binding domains (CaMBD) are present in all TRP genes within the carboxy terminus (22). TRPC4α contains two CaMBD, but in TRPC4β the second CaMBD is deleted due to alternative splicing. These cDNAs, isolated from mouse colonic smooth muscle RNA, share complete amino acid identity in the CaMBD to those previously reported in mouse brain (22).

Native inward current in HEK-293 cells. We investigated native currents in nontransfected HEK-293 cells and in HEK-293 cells infected with a virus expressing only GFP to determine the extent of endogenous TRP currents in this expression system. We detected transcripts for TRPC4α and TRPC4β in HEK cells (data not shown) similar to other investigators (27).

With the use of the whole cell patch-clamp technique, cells were dialyzed with BAPTA solutions (10 mM, reducing intracellular free Ca^{2+} to ~10 nM; see MATERIALS AND METHODS). This caused development of inward current that reached a steady state within 5–7 min after breaking into the whole cell configuration. This native inward current in GFP-transfected cells averaged −54.8 ± 19.6 pA at a holding potential of −60 mV ($n = 5$, Fig. 1*A*). The internal solution was designed to set E_{Cl} at ~−30 mV.

The effects of CMZ, a calmodulin inhibitor, were tested on the endogenous currents in HEK cells. The cells were dialyzed with EGTA (0.1 mM, reducing in-

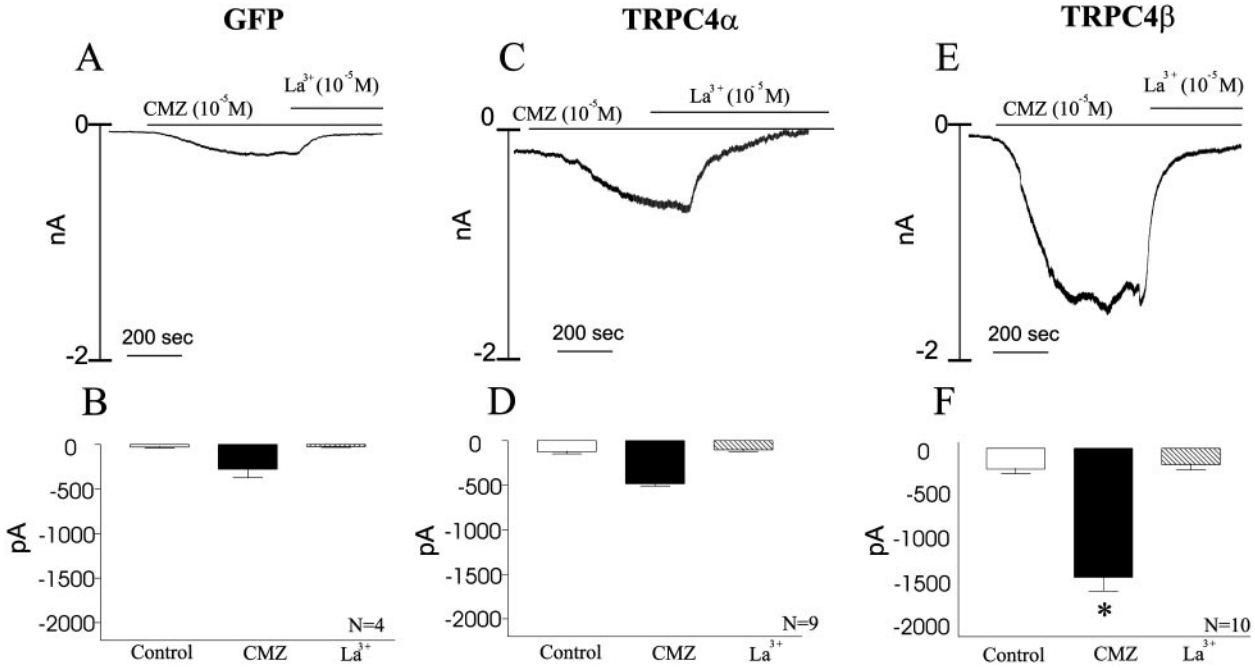

Fig. 2. Effect of calmidazolium (CMZ) on TRPC4α and TRPC4β expressed in HEK-293 cells. EGTA (0.1 mM) was used for dialysis on cells to study the effects of CMZ. *A*: the effect of CMZ (10 μM) in these control cells showing a slight increase in the current that could be blocked by application of 10 μM $LaCl_3$ (La^{3+}). Data for control HEK cells are summarized in *B*. *C* and *D*: the current generated in HEK cells infected with TRPC4α virus. In *C*, dialysis with 0.1 mM EGTA generates a slightly larger current in these cells compared with control HEK cells, but smaller than cells expressing TRPC4β. Summarized data for TRPC4α currents are shown in *D*. *E* and *F*: the current generated in HEK cells stably transfected with TRPC4β. Application of CMZ on these cells leads to a significant increase in the inward current that is also sensitive to block by La^{3+}. Summarized data for TRPC4β currents are shown in *F*. *Statistically significant difference between TRPC4β and GFP-transfected cells, $P < 0.01$.

tracellular free Ca^{2+} to ~100 nM). Dialysis of cells with this buffer strength failed to elicit tonic inward currents, as observed when cells were dialyzed with 10 mM BAPTA. Application of CMZ (10^{-5} M) increased inward currents from −28 ± 10 to −278 ± 94 pA (n = 4, Fig. 2*A*). The CMZ-sensitive current was restored approximately to control levels (e.g., −23 pA) by application of 10 μM lanthanum (La^{3+}), a nonselective blocker of cation channels including TRP channels (5). Summarized data for native currents in HEK cells are shown in Figs. 1*D* and 2*B*. These experiments confirm that HEK cells have native, nonselective cation currents, as previously demonstrated (27, 28).

Expression of TRPC4α in HEK-293 cells. Currents were recorded from HEK cells stably transfected with TRPC4α and TRPC4β or infected with similarly constructed adenovirus. To determine the calcium regulation of these TRP channels, cells were dialyzed with BAPTA (10 mM), which activated an inward current in cells expressing TRPC4α averaging −618 ± 239 pA at −60 mV; n = 6, $P < 0.05$ (Fig. 1*B*). Summarized data are shown in Fig. 1*D*. Inward currents were of smaller

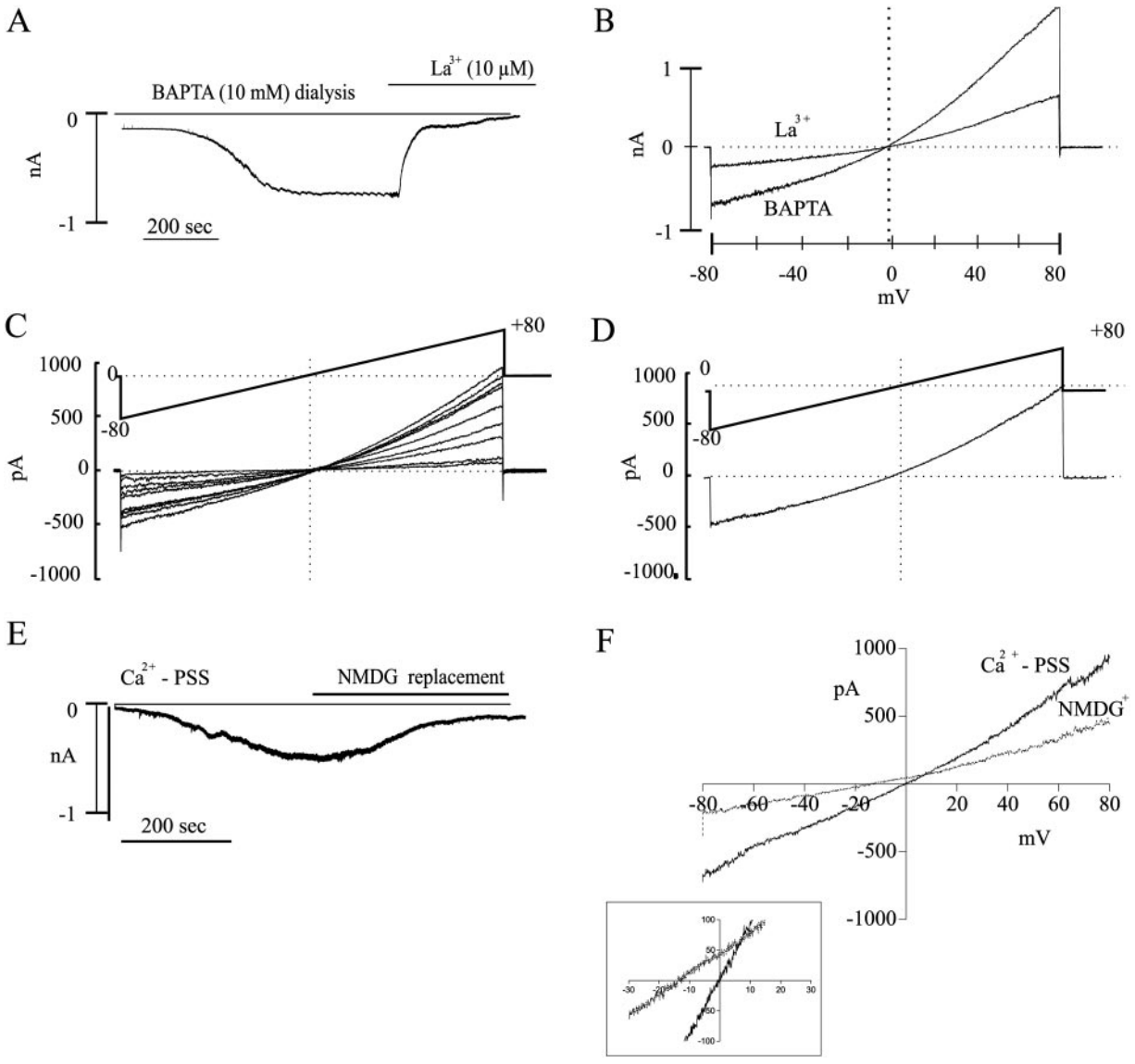

Fig. 3. Cation selectivity of TRPC4β; effect of *N*-methyl-D-glucamine (NMDG) replacement. Currents were recorded by using the whole cell patch-clamp technique; holding potential −60 mV. *A*: dialysis with 10 mM BAPTA generates a large current in HEK-293 cells expressing TRPC4β that is sensitive to block with 10 μM La^{3+}. A ramp protocol from −80 to +80 mV shown in *B* was used to demonstrate the characteristics of the La^{3+} block in these cells. La^{3+} blocked both the inward and outward currents in these cells without changing the reversal potential. *C*: the development of the BAPTA-activated current in 30-s intervals. *D*: the difference current before and after full dialysis of 10 mM BAPTA. *E* and *F*: the effect of replacing Na^+ with NMDG after development of the current during BAPTA dialysis. *E*: a representative trace of NMDG replacement while holding the cell at −60 mV. A significant decrease in the current was noted, as was a shift in the reversal potential toward more negative potentials. (n = 4, $P < 0.01$). *Inset* in *F* shows a closer look at the reversal potential shift.

magnitude in TRPC4α cells dialyzed with 0.1 mM EGTA (−125 ± 23 pA; $n = 9$, $P < 0.01$) than in cells dialyzed with BAPTA at a holding potential of −60 mV (compare control in Fig. 2, *C* and *D*, to Fig. 1, *B* and *D*). After full development of current after dialysis with EGTA (0.1 mM), CMZ (10 μM) increased the inward current to −482 ± 27 pA at −60 mV ($n = 9$). La^{3+} blocked the inward current to control levels (Fig. 2, *C* and *D*). Summarized data are shown in Fig. 2*D*.

Expression of TRPC4β in HEK-293 cells. Dialysis of cells expressing TRPC4β with BAPTA (10 mM) induced inward currents within 5–10 min after establishing the whole cell configuration (Fig. 1*C*). The inward current activated by BAPTA was significantly increased (−691 ± 134 pA at −60 mV; $n = 16$, $P < 0.05$) compared with control, untransfected cells, or cells infected with a virus expressing only GFP. Other cells were dialyzed with 0.1 mM EGTA. At a holding potential of −60 mV, currents in these cells were smaller (e.g., −233 ± 53 pA; $n = 10$, $P < 0.05$, control in Fig. 2, *E* and *F*) than in BAPTA dialyzed cells. These data demonstrate that cells expressing TRPC4α and TRPC4β have a current available that is inhibited by Ca^{2+}.

Application of CMZ to TRPC4β-expressing cells dialyzed with 0.1 mM EGTA induced a significantly larger inward current compared with GFP-transfected cells (−1,458 ± 156 pA; $P < 0.01$, $n = 10$, Fig. 2, *E* and *F*). The current activated by CMZ was inhibited by La^{3+} (10 μM, −184 ± 57 pA; $n = 10$, Fig. 2, *E* and *F*). Summarized data are shown in Fig. 2*F*. Similar results were seen using HEK cells transiently transfected with an adenovirus expressing TRPC4β (data not shown). These data suggest that TRPC4α is less responsive to antagonizing calmodulin binding by CMZ than TRPC4β.

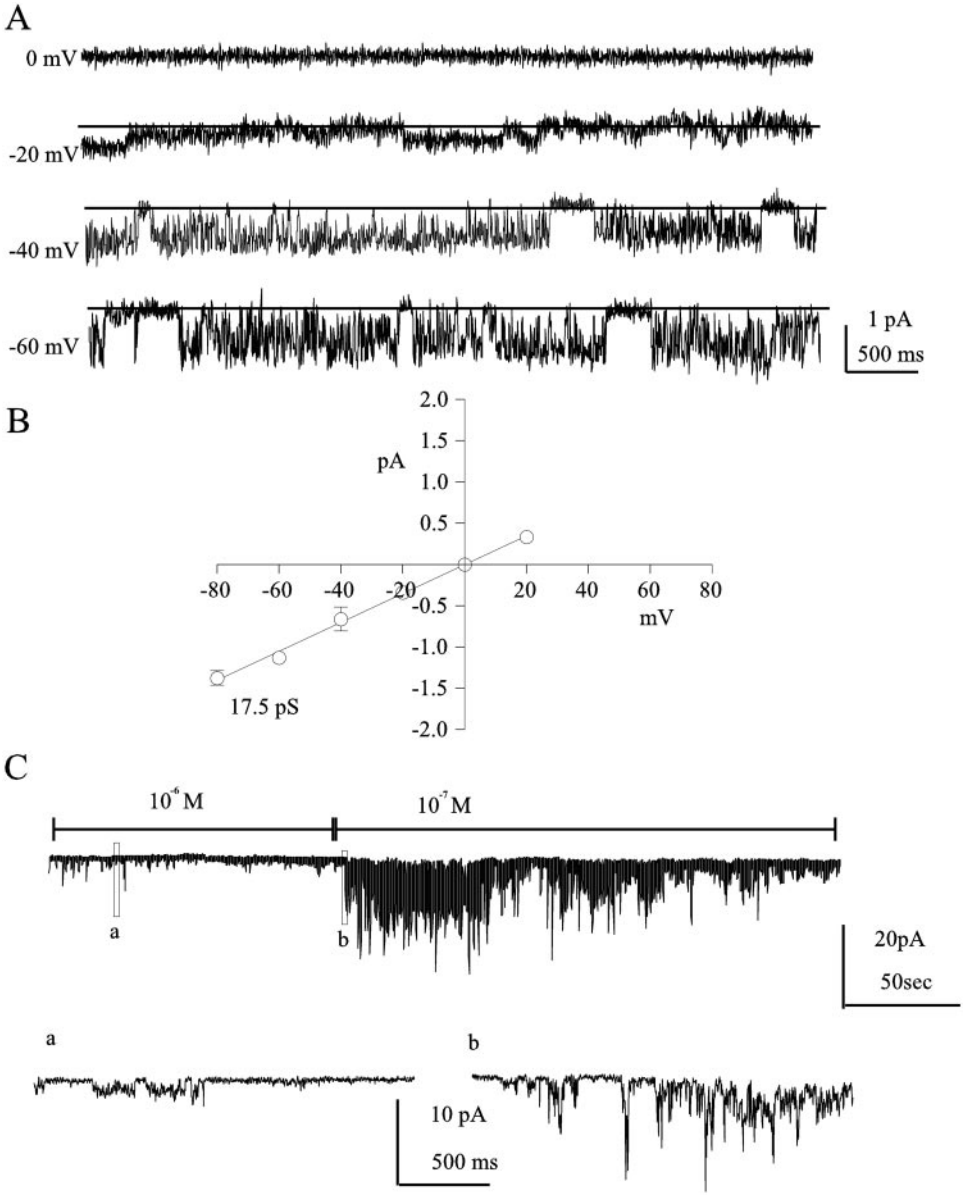

Fig. 4. Unitary currents recorded from HEK-293 cells expressing TRPC4β. *A*: the effect of voltage on unitary currents in a cell attached patch exposed to 10^{-6} calcium. Solid line indicates when the channels are closed. At voltages +20 mV, the currents became too noisy to record single-channel events. Recordings obtained at potentials from −60 to +20 mV are shown. *B*: data from 3 cells are plotted and the average current-voltage relationship is shown. For some points, the error bars are contained within the symbols. Fitting the averaged data points by linear regression shows a unitary current due to a 17.5 pS conductance. *C*: the reverse calcium dependence of TRPC4β in an excised patch exposed to 10^{-6} M and 10^{-7} M calcium. *Insets* show segments of the recording at faster time sweeps and an expanded scale.

Cation selectivity of TRPC4β currents in HEK-293 cells. Inward current generated in TRPC4β cells by BAPTA dialysis were also blocked by 10 μM La^{3+} (−691 ± 134 to −108 ± 22 pA; $n = 5$, Fig. 3, *A* and *B*), as observed with currents activated by 0.1 mM EGTA dialysis. By using a ramp protocol (from −80 to +80 mV), the inward currents were activated by BAPTA without a change in reversal potential throughout development (Fig. 3*C*). Application of La^{3+} inhibited the BAPTA-induced current and also did not result in a change in the reversal potential (Fig. 3*B*). The current activated by BAPTA dialysis was reduced by replacement of external Na^+ with NMDG. This reduced the inward current from −471.4 ± 74 to −142 ± 25 pA (−60 mV; $n = 4$, $P < 0.05$, Fig. 3, *E* and *F*) and shifted the reversal potential from −1 ± 0.3 to −14 ± 0.8 mV ($P < 0.01$, Fig. 3, *E* and *F*; see *inset* of 3*F*).

Effects of niflumic acid and DIDS on TRPC4β currents. Niflumic acid and DIDS have been shown to block the Ca^{2+}-inhibited, nonselective cation currents in ICC (10). Therefore, we tested the effects of niflumic acid on HEK-293 cells stably expressing TRPC4β. In these experiments, currents were evoked by application of 10^{-5} M CMZ. Niflumic acid (30 μM) reduced the amplitude of the inward current from −1,438 ± 273 to −247 ± 141 pA, ($n = 6$, $P < 0.05$). Use of a ramp protocol demonstrated that application of niflumic acid did not cause a change in the reversal potential, although the current at all potentials was decreased. A similar pharmacological effect was noted with application of 100 μM DIDS reducing the amplitude of the inward current from −809 ± 129 to −274 ± 97 pA, ($n = 4$, $P < 0.05$).

Unitary currents in HEK-293 cells expressing TRPC4β. We further investigated the properties of TRPC4β currents at the single-channel level. Unitary currents were recorded in on-cell patches in TRPC4β expressing cells as the membrane potential of the patch was stepped to various potentials. Recordings at potentials positive to +20 mV were too noisy to clearly discern single-channel currents, so current-voltage curves were generated for potentials between −60 and +20 mV (Fig. 4*A*). The averaged data from 5 cells revealed a single-channel conductance of 17.5 ± 0.5 pS (Fig. 4*B*). A whole cell current was activated and shown to reverse at 0 mV when cells were dialyzed with 10 mM BAPTA. These observations suggested to us that reduced cytoplasmic Ca^{2+} may activate these channels. To test the properties of the channels more directly, patches were excised, allowing the interior of the patch to be exposed to bathing solutions containing 10^{-6} M Ca^{2+} (pipette solution contained Ca^{2+}-PSS; E_K and E_{Cl} were −87 and −30 mV, respectively). We examined the reverse calcium dependence of the unitary current using a cell-excised patch exposed to 10^{-6} M calcium (Fig. 4*C*). The open probability of the channel was greatly increased upon exposure to 10^{-7} M calcium (Fig. 4*C*).

Under whole cell conditions, the application of CMZ activated TRPC4β currents (Fig. 2, *E* and *F*). Therefore, additional experiments were performed on the single-channel currents in on-cell and excised patches. Application of CMZ (10 μM) during measurement of single-channel currents in on-cell patches greatly increased channel activity and made it difficult to resolve unitary currents at a −60 mV holding potential (Fig.

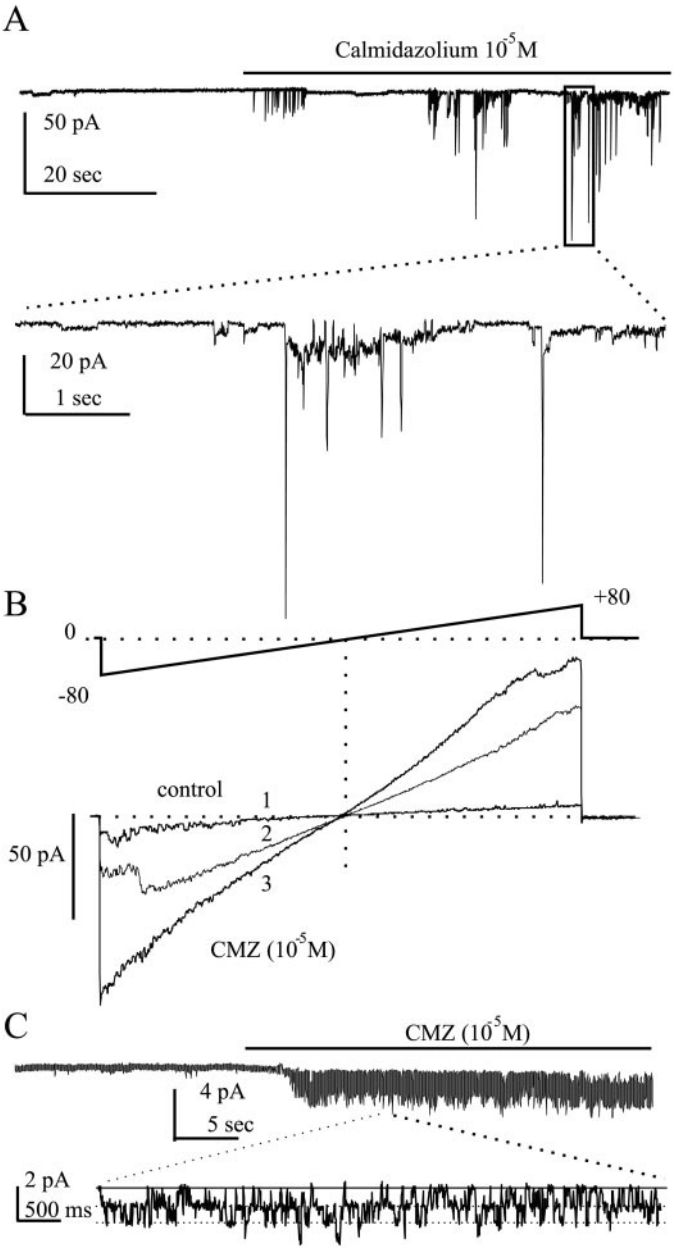

Fig. 5. Effect of CMZ on TRPC4β single-channel events. *A*: the effect of 10 μM CMZ on an on-cell patch from HEK-293 cells stably expressing TRPC4β. Recordings from *A* at faster time sweeps and an expanded scale are shown below bordered by dotted lines. The application of CMZ increased both the amplitude and frequency of single-channel currents. *B*: increased single-channel activity after CMZ exposure using a ramp protocol (see *inset*). *1*, control levels before CMZ exposure; *2*, 30 s after application of CMZ; *3*, 60 s after application of CMZ. *C*: the effect of CMZ on an excised patch exposed to 10^{-6} M calcium. *Inset* shows a portion of the recording from *C* at a faster time sweep. After application of CMZ, single-channel events were greatly increased. At least 3 channels were present in the patch. The dotted line denotes the 0 current level.

5*A*). Ramp protocols (−80 to +80 mV) were also performed while applying CMZ. CMZ increased the number of channel openings (increased slopes) without changing the reversal potential (from −0.4 ± 0.1 to −0.5 ± 0.1 mV; Fig. 5*B*, $n = 5$). The effect of CMZ on excised patches was also tested (Fig. 5*C*). When the cytosolic surface was exposed to 10 μM CMZ, the channel openings were greatly increased at a holding potential of −60 mV. Unitary currents were more easily discernable at faster time sweeps and larger scales as shown in the subset of Fig. 5, *A* and *C*.

DISCUSSION

In the present study, we have evaluated currents expressed in HEK-293 cells after transfection of the cells with TRPC4 splice variants. We found that buffering Ca^{2+} to low levels within the cells results in the activation of persistent inward currents that reverse at ~0 mV and are reduced in amplitude by replacing Na^+ with $NMDG^+$. TRPC4 currents could also be induced by treating cells with CMZ, a calmodulin inhibitor. Previous studies have shown that Ca^{2+}/calmodulin binding to TRPC3 and TRPC4 channels causes inhibition of the intrinsically high open probability of these channels (19, 30). Work by Zhang et al. (30) demonstrated that TRPC3 bound Ca^{2+}/calmodulin at a site that overlapped with the IP_3 receptor (IP_3R) binding domain and could be activated by CMZ. Tang et al. (19) went further to show that other TRP proteins, including TRPC4, could also interact with IP_3R and calmodulin, but that one such site present in TRPC4α was absent in TRPC4β. Given this observation, we addressed this difference by examining the functional properties of the two TRPC4 splice variants at a whole cell and single-channel level. Some properties of TRPC4α and TRPC4β were different between our study and that of Schaefer et al. (17), including the double rectification observed at very negative and positive potentials and the single-channel conductance (30 pS). This may be due to differences in recording conditions or solutions used during recording.

The single-channel conductance of expressed TRPC4β channels was 17.5 pS, and these channels were inhibited by Ca^{2+}. Channel openings with the same characteristics were activated in on-cell patches and in excised patches by CMZ. These properties are similar to the properties of the conductance in native ICC that is responsible for the pacemaker current (see Table 1 for a comparison of the currents). ICC express TRPC4 isoforms at the transcriptional level, and a recent study showed immunochemical evidence suggesting TRPC4 expression, particularly in caveolae, in ICC (20). Immunochemical staining of TRPC4 was also detected within putative smooth muscle cells in these same preparations; however, the TRPC4 expression was clearly stronger in the colabeled ICC than in the other cell types (20). This observation suggests that a decreased translation of the TRPC4 protein within smooth muscle cells could explain the lack of a Ca^{2+}-inhibited current within these cells. Taken together, these data suggest that TRPC4 or TRPC4-like channels might encode the pacemaker conductance in ICC.

Transcripts of TRPC6 have also been identified in ICC (1). Experiments with BAPTA dialysis in HEK-293 cells stably transfected with TRPC6, however, failed to generate a current similar to that seen in TRPC4β-transfected cells or in ICC (24). A recent study has shown that TRPC4 is predominantly expressed in ICC, whereas smooth muscle cells in the same preparation predominantly express TRPC6 (20). TRP channels can form heterotetramers with slightly different properties to the homotetrameric channels (12, 29). A recent study demonstrates that heterotetramers can form between TRPCs 1, 4, and 5 or TRPCs 3, 6, and 7, but not between the two channel subgroups (3, 6, 18). Thus, as TRPC1 and TRPC5 have not been identified in ICC, it is reasonable to assume that TRPC4 forms a homotetramer in ICC, although channels consisting of TRPC4α and TRPC4β cannot be ruled out.

Although ICC have Ca^{2+}-inhibited, nonselective cation channels (10), a similar conductance was not detected in intestinal smooth muscle cells in spite of the fact that transcripts for TRPC4 have been found in vascular and visceral smooth muscle cells (1, 23). Both ICC and smooth muscle cells contain transcripts for each splice variant, with TRPC4β dominating in quantitative studies involving tissue from different regions of the GI tract, including tissue obtained from mouse intestine (23). In addition, murine and canine fundus smooth muscles, electrically quiescent tissues, expressed the TRPC4α isoform predominantly as opposed to TRPC4β in isolated smooth muscle cells (23).

Table 1. *Comparison of the functional properties of expressed TRPC4β in HEK-293 cells and the native calcium-inhibited nonselective cation channel in ICC*

	ICC Nonselective Cation Channel	TRPC4β
Calmidazolium sensitivity	Activated strongly	Activated strongly
Pharmacological blockers	Lanthanides; niflumic acid; DIDS	Lanthanides; niflumic acid; DIDS
Single-channel conductance, pS	13	17.5
Calcium regulation	Strongly activated by 10^{-7} Ca^{2+}; 10^{-6} reduces activity	Strongly activated by 10^{-7} Ca^{2+}; 10^{-6} reduces activity
Reversal potential, mV	0	0
NMDG replacement shift, mV	14.6	13

Interstitial cells of Cajal (ICC) nonselective cation channel data are from Ref. 9. NMDG, *N*-methyl-D-glucamine.

Interestingly, neither BAPTA dialysis nor application of CMZ on freshly dispersed smooth muscle cells from mouse ileum (n = 45; unpublished observations) yielded a current comparable to that seen in cultured ICC or HEK cells expressing TRPC4α or TRPC4β. A recent study from Schaefer et al. (17) suggested that TRPC4α is capable of forming heterotetramers with TRPC4β and works in a dominant negative fashion to inhibit the currents generated from expression of TRPC4β homotetramers. It is possible that the function of TRPC4β in smooth muscle cells is altered by the presence of other TRP isoforms or is possibly inhibited by the expression of TRPC4α and that cells predominantly expressing TRPC4α display little current from the heterotetrameric channels.

Electrical slow waves are a fundamental property of phasic GI muscles, and these events activate periodic Ca^{2+} entry and regulate contractions in electrically coupled smooth muscle cells. A Ca^{2+}-inhibited, nonselective cation conductance contributes to the pacemaker current that initiates slow wave activity (10, 11). In the present study, we identified a molecular entity, TRPC4, that shares many similarities with native pacemaker channels. We have demonstrated that a splice variant of TRPC4 (TRPC4β) that eliminates a calmodulin-binding site in the carboxy terminus of channels generates robust currents when intracellular Ca^{2+} is decreased or calmodulin inhibitors are applied. The preponderance of circumstantial evidence leads us to suggest that TRPC4β or a TRPC4β-like channel encodes the pacemaker conductance in ICC. These experiments have not ruled out the possibility that an as yet unidentified TRP channel may be responsible for encoding the plasmalemmal pacemaker current in murine small intestine. However, we have demonstrated that if an unknown conductance exists and is involved in pacemaking, it must have properties very similar to TRPC4. Thus we would conclude that the pacemaker current in ICC is either a TRPC4 conductance or a TRPC4-like conductance.

We thank L. Miller and H. Beck for excellent technical assistance.

The National Institute of Diabetes and Digestive and Kidney Diseases Grant DK-41315 supported this work. R. L. Walker is a predoctoral fellow of the American Heart Association-Western States Affiliate.

REFERENCES

1. **Epperson A, Hatton WJ, Callaghan B, Doherty P, Walker RL, Sanders KM, Ward SM, and Horowitz B.** Molecular markers expressed in cultured and freshly isolated interstitial cells of Cajal. *Am J Physiol Cell Physiol* 279: C529–C539, 2000.
2. **Freichel M, Suh SH, Pfeifer A, Schweig U, Trost C, Weissgerber P, Biel M, Philipp S, Freise D, Droogmans G, Hofmann F, Flockerzi V, and Nilius B.** Lack of an endothelial store-operated Ca^{2+} current impairs agonist-dependent vasorelaxation in TRP4 −/− mice. *Nat Cell Biol* 3: 121–127, 2001.
3. **Goel M and Schilling WP.** Association of immunophilins with mammalian TRP channels (Abstract). *Biophysical Journal* 82: 637a, 2002.
4. **Groschner K, Hingel S, Lintschinger B, Balzer M, Romanin C, Zhu X, and Schreibmayer W.** Trp proteins form store-operated cation channels in human vascular endothelial cells. *FEBS Lett* 437: 101–106, 1998.
5. **Halaszovich CR, Zitt C, Jungling E, and Luckhoff A.** Inhibition of TRP3 channels by lanthanides. Block from the cytosolic side of the plasma membrane. *J Biol Chem* 275: 37423–37428, 2000.
6. **Hofmann T, Schaefer M, Schultz G, and Gudermann T.** Subunit composition of mammalian transient receptor potential channels in living cells. *Proc Natl Acad Sci USA* 99: 7461–7466, 2002.
7. **Huizinga JD, Robinson TL, and Thomsen L.** The search for the origin of rhythmicity in intestinal contraction; from tissue to single cells. *Neurogastroenterol Motil* 12: 3–9, 2000.
8. **Jungnickel MK, Marrero H, Birnbaumer L, Lemos JR, and Florman HM.** Trp2 regulates entry of Ca^{2+} into mouse sperm triggered by egg ZP3. *Nat Cell Biol* 3: 499–502, 2001.
10. **Koh SD, Jun JY, Kim TW, and Sanders KM.** A Ca^{2+}-inhibited nonselective cation conductance contributes to pacemaker currents in mouse interstitial cell of Cajal. *J Physiol* 540: 803–814, 2002.
11. **Koh SD, Sanders KM, and Ward SM.** Spontaneous electrical rhythmicity in cultured interstitial cells of Cajal from the murine small intestine. *J Physiol* 513: 203–213, 1998.
12. **Lintschinger B, Balzer-Geldsetzer M, Baskaran T, Graier WF, Romanin C, Zhu MX, and Groschner K.** Coassembly of Trp1 and Trp3 proteins generates diacylglycerol- and Ca^{2+}-sensitive cation channels. *J Biol Chem* 275: 27799–27805, 2000.
13. **Mery L, Magnino F, Schmidt K, Krause KH, and Dufour JF.** Alternative splice variants of hTrp4 differentially interact with the C-terminal portion of the inositol 1,4,5-trisphosphate receptors. *FEBS Lett* 487: 377–383, 2001.
14. **Montell C.** Physiology, phylogeny, and functions of the TRP superfamily of cation channels. *Sci STKE* 2001: RE1, 2001.
15. **Philipp S, Cavalie A, Freichel M, Wissenbach U, Zimmer S, Trost C, Marquart A, Murakami M, and Flockerzi V.** A mammalian capacitative calcium entry channel homologous to *Drosophila* TRP and TRPL. *EMBO J* 15: 6166–6171, 1996.
16. **Sanders KM.** A case for interstitial cells of Cajal as pacemakers and mediators of neurotransmission in the gastrointestinal tract. *Gastroenterology* 111: 492–515, 1996.
17. **Schaefer M, Plant TD, Stresow N, Albrecht N, and Schultz G.** Functional differences between TRPC4 splice variants. *J Biol Chem* 277: 3752–3759, 2002.
18. **Strubing C, Krapivinsky G, Krapivinsky L, and Clapham DE.** TRPC1 and TRPC5 form a novel cation channel in mammalian brain. *Neuron* 29: 645–655, 2001.
19. **Tang J, Lin Y, Zhang Z, Tikunova S, Birnbaumer L, and Zhu MX.** Identification of common binding sites for calmodulin and inositol 1,4,5-trisphosphate receptors on the carboxyl termini of trp channels. *J Biol Chem* 276: 21303–21310, 2001.
20. **Torihashi S, Fujimoto T, Trost C, and Nakayama S.** Calcium oscillation linked to pacemaking of interstitial cells of Cajal: requirement of calcium influx and localization of TRP4 in caveolae. *J Biol Chem* 277: 19191–19197, 2002.
21. **Torihashi S, Nishi K, Tokutomi Y, Nishi T, Ward S, and Sanders KM.** Blockade of kit signaling induces transdifferentiation of interstitial cells of cajal to a smooth muscle phenotype. *Gastroenterology* 117: 140–148, 1999.
22. **Trost C, Bergs C, Himmerkus N, and Flockerzi V.** The transient receptor potential, TRP4, cation channel is a novel member of the family of calmodulin binding proteins. *Biochem J* 355: 663–670, 2001.
23. **Walker RL, Hume JR, and Horowitz B.** Differential expression and alternative splicing of TRP channel genes in smooth muscles. *Am J Physiol Cell Physiol* 280: C1184–C1192, 2001.
24. **Walker RL, Koh SD, Greenwood IA, Sergeant GP, and Horowitz B.** Functional characterization of smooth muscle TRP channels using an adenoviral expression system (Abstract). *Biophysical Journal* 82: 422a, 2002.
25. **Ward SM, Burns AJ, Torihashi S, and Sanders KM.** Mutation of the proto-oncogene c-kit blocks development of interstitial cells and electrical rhythmicity in murine intestine. *J Physiol* 480: 91–97, 1994.
26. **Ward SM, Ordog T, Koh SD, Baker SA, Jun JY, Amberg G, Monaghan K, and Sanders KM.** Pacemaking in interstitial cells of Cajal depends upon calcium handling by endoplasmic reticulum and mitochondria. *J Physiol* 525: 355–361, 2000.

27. **Wu X, Babnigg G, and Villereal ML.** Functional significance of human TRP1 and TRP3 in store-operated Ca^{2+} entry in HEK-293 cells. *Am J Physiol Cell Physiol* 278: C526–C536, 2000.
28. **Wu X, Babnigg G, Zagranichnaya T, and Villereal ML.** The role of endogenous human trp4 in regulating carbachol-induced calcium oscillations in HEK-293 cells. *J Biol Chem* 277: 13597–13608, 2002.
29. **Xu XZ, Li HS, Guggino WB, and Montell C.** Coassembly of TRP and TRPL produces a distinct store-operated conductance. *Cell* 89: 1155–1164, 1997.
30. **Zhang Z, Tang J, Tikunova S, Johnson JD, Chen Z, Qin N, Dietrich A, Stefani E, Birnbaumer L, and Zhu MX.** Activation of Trp3 by inositol 1,4,5-trisphosphate receptors through displacement of inhibitory calmodulin from a common binding domain. *Proc Natl Acad Sci USA* 98: 3168–3173, 2001.